Different reverse leakage current transport mechanisms of planar Schottky barrier diodes(SBDs) on sapphire and GaN substrate

Xiao Wang [a,b], Zhi-Yu Lind [d], Yu-Min Zhang [b,c], Jian-Feng Wang [b,*], Ke Xu [b,c,d,*]

[a] School of Nano-Tech and Nano-Bionics, University of Science and Technology of China, Hefei, 230026, Anhui, China
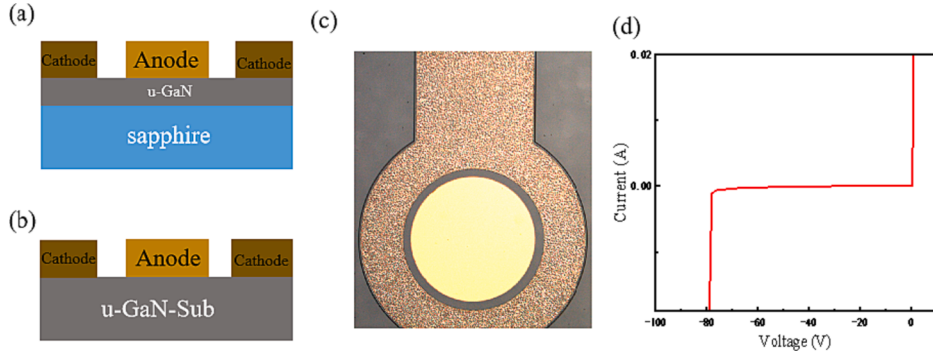[b] Suzhou Institute of Nano-tech and Nano-bionics, Chinese Academy of Sciences, Suzhou, 215123, Jiangsu, China
[c] Suzhou Nanowin Science and Technology Co, Ltd., Suzhou, 215123, Jiangsu, China
[d] Shenyang National Laboratory for Materials Science, Jiangsu Institute of Advanced Semiconductors, Suzhou, 215123, Jiangsu, China

ABSTRACT

The effects of different substrates on the off-state leakage current in gallium nitride (GaN) planar diodes are experimentally demonstrated and studied by analyzing temperature-dependent current–voltage characteristics. The two devices exhibit different leakage mechanisms despite being subjected to the same process conditions. The device with a sapphire substrate shows a more intricate leakage mechanism, implying the presence of additional leakage channels compared to the device with free-standing substrates. The electrical leakage characteristics in the planar GaN-on-sapphire device (referred to as utemp-SBD) and GaN substrate device (referred to as usub-SBD) Schottky barrier diodes (SBD) can be described by two distinct processes as the reverse bias gradually increases: utemp-SBD go through the thermionic emission (TE), variable range hopping (VRH), Frenkel–Poole (FP) emission and space-charge-limited conduction (SCLC) model; The leakage conduction mechanism of usub-SBD include TE, VRH, and FP emission mechanisms. It is noteworthy that in device 1, there is a rapid increase in leakage current within the voltage range of −36 to −40 V, primarily driven by the SCLC mechanism. This effect arises due to the presence of intrinsic traps in GaN grown on a heterogeneous substrate. Additionally, in the voltage range of −7 to −50 V (348 K to 448 K), the leakage mechanism shifts from FP emission to the VRH model, possibly due to variations in the Schottky barrier height.This study provides an in-depth analysis of the leakage mechanisms observed on different substrates and offers valuable insights for the design of planar gate transistors to minimize or avoid the occurrence of leakage channels.

Introduction

As the third generation semiconductor material, gallium nitride material has great performance advantages, including high saturated electron drift velocity, high theoretical breakdown field strength, physical stability, large band-gap width and adjustable bandwidth [1–3]. Gallium nitride-based power devices with high output power, high frequency, excellent thermal management and stable dynamic characteristics have attracted much attention [4–10]. These devices can be classified into two primary categories: vertical and planar structures. Vertical power devices possess advantages in terms of on-resistance, breakdown voltage, and device size design [11]. The current commercial GaN devices mainly focus on Schottky barrier diode (SBD) and high electron mobility transistor (HEMT) [11]. However, SBDs exhibit a larger leakage current due to their low barrier height compared to other

power devices, and the Schottky gate leakage in HEMT devices remains a critical parameter for improving device reliability [12,13]. In the field of microwave applications, gate leakage significantly impacts the noise performance of AlGaN/GaN high electron mobility transistors (HEMTs) [14]. In power devices, leakage current results in additional power losses and reduces device efficiency [15]. Dislocations serve as the primary pathway for leakage current [16,17]. Due to its low dislocation density, the free-standing GaN substrate has the great potential to suppress leakage and enhance the performance of GaN-based devices. In addition, the application of GaN power devices has covered the low, medium and high voltage stages, and they operate in high-temperature conditions. Therefore, for different dislocation density on different substrate, it is necessary to systematically measure the temperature-related current and voltage characteristics of Schottky barrier diodes and study their leakage conduction mechanisms.

Fig. 1. (a),(b) Schematic diagram of the planar GaN-on-sapphire (utemp-SBD) and GaN substrate (usub-SBD) Schottky barrier diodes; (c) Optical diagram of the device; (d) Schottky rectification characteristic IV curve.
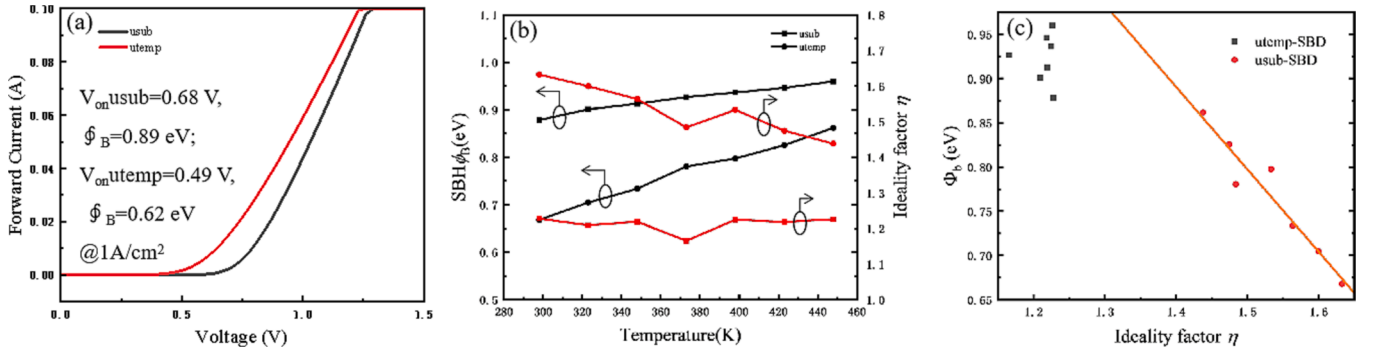
Fig. 2. (a) Forward I–V characteristics in a linear-scale; (b) Extracted SBH and η versus T using single-temperature I − V method; (c) is the relationship between SBH and η.

The conduction mechanism of planar GaN SBD leakage current on different substrates has been limited in previous studies. Zhang et al. reported that variable range hopping (VRH) on gallium nitride vertical diodes is the primary reverse leakage mechanism on all Si, sapphire and gallium nitride substrate [18,19]. Recently, Guo et al. found that the main leakage mechanism varies at different voltages and also differs between devices with and without implantation termination [20]. Chen investigated the leakage current transmission mechanism of quasi-vertical silicon Schottky barrier diodes (SBDs) under low and high reverse bias and different temperatures [21]. A few studies on the leakage conduction mechanism of Schottky diodes primarily focus on GaN-on-Si vertical and quasi-vertical SBDs [21].

In this work, we reveal the different reverse bias leakage conduction mechanisms of the planar GaN-on-sapphire (utemp-SBD) and GaN substrate (usub-SBD) Schottky barrier diodes. We provide a systematic and comprehensive explanation of the physical mechanisms underlying the different leakage conduction mechanisms observed on the two substrates.

Device structure and fabrication

As shown in Fig. 1(a) and (b), the utemp-SBD consists of a 4.5-μm-thick high-quality N-drift layer deposited on a sapphire substrate by metal–organic chemical deposition (MOCVD) (N_D-N_A ~ 1.7×10^{16} cm^{-3}, dislocation density is 1×10^9 cm^{-2}), usub-SBD is fabricated by directly depositing electrodes directly on an undoped substrate of GaN (N_D ~ 5×10^{16} cm^{-3}, dislocation density is 9.1×10^6 cm^{-2}) grown via Hydride vapor epitaxial deposition (HVPE). Ti/Al/Ni/Au (20/130/50/150 nm) Ohmic electrode were deposited by electron beam evaporation and annealed at 870 °C for 30 s in nitrogen. The Ni/Au (50/130 nm) were deposited to form Schottky anode. The circular anode has a diameter of 460 μm, The distance between the anode pad and cathode pad is 20 μm.

Both devices do not have any terminal structure or surface treatment. The optical diagram of the device is shown in Fig. 1(c). Usub-SBD I-V curve is shown in Fig. 1(d), the device has good Schottky I-V curve characteristics and the breakdown voltage of the device on the substrate is about 80 V.

Results and discussion

Fig. 2(a) shows the linear-scale plot of the forward I–V curves of both devices. In general, the forward conduction performance of the Schottky contact is dominated by the thermionic emission (TE) mechanism, which can be expressed as [20]

$$J = J_S \times exp(\frac{qV}{\eta kT})[1 - exp(\frac{-qV}{kT})] \qquad (1)$$

$$J_s = A^* T^2 exp(-\frac{q\varnothing_B}{kT}) \qquad (2)$$

where J, J_S, k, T, q, V, A^* and ϕ_B are the current density, saturation current density, Boltzmann's constant, temperature, electron charge, voltage across Schottky junction, Richardson's constant and SBH, respectively. The extracted Schottky barrier height (SBH) $\varnothing_B$ of the utemp-SBD and usub-SBD are 0.62 eV and 0.89 eV at a forward current density of 1A/cm^2, respectively. Under The same process conditions and similar doping concentration, the utemp-SBD shows that lower Schottky barrier height may be related to high dislocation density. Impurity aggregation near the dislocation leads to a higher concentration of donor surface states, the reduced energy level of the localized conduction band is the primary element leading to the observed lower Schottky barrier height [22,23]. Through the variable temperature I-V test, we extracted the barrier heights and the ideality factor (η) at different temperatures
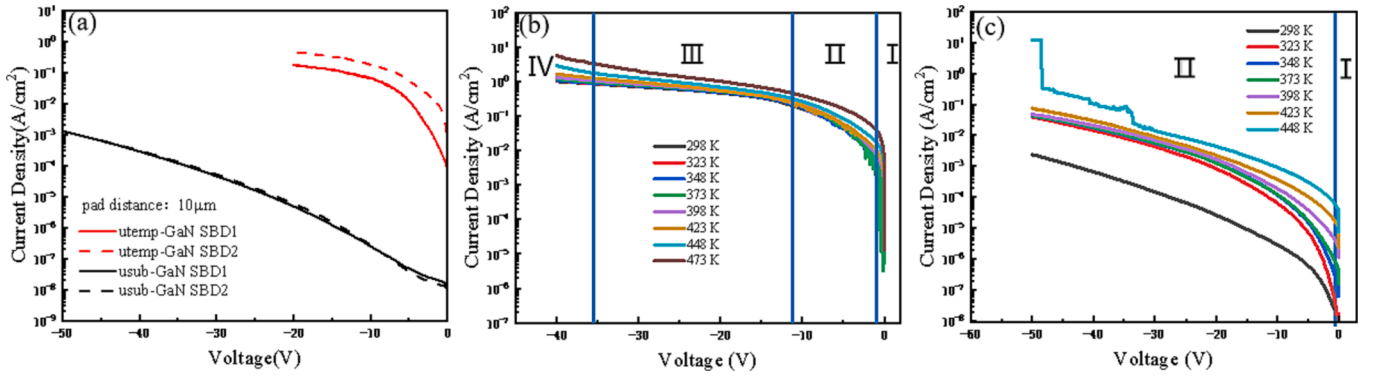
Fig. 3. (a) Reverse I-V characteristics on different substrate at room temperature; (b),(c) Temperature-dependent reverse I-V characteristics of the fabricated utemp-SBD and usub-SBD with T varying from 298 to 448 K.
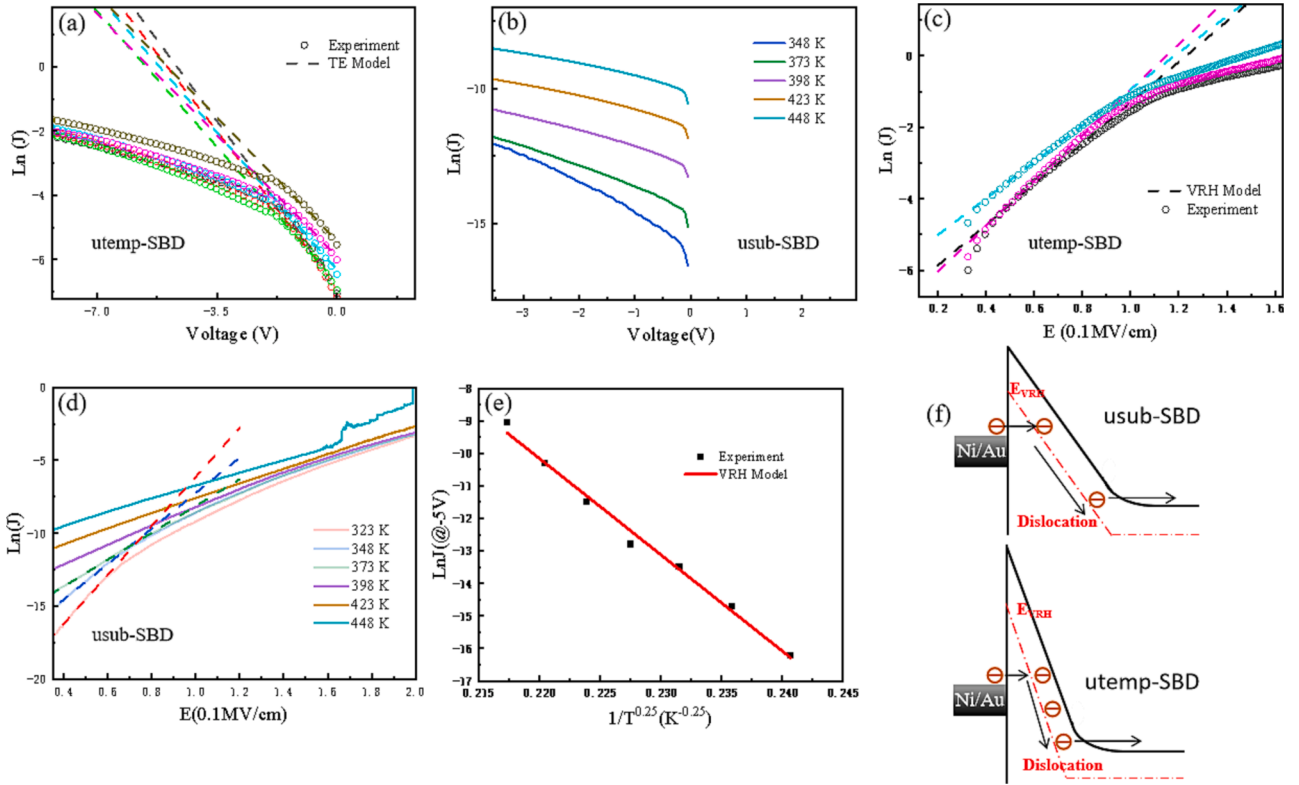
Fig. 4. (a),(b) Reverse ln(J) versus V for utemp-SBD and usub-SBD, respectively; ln(J) as a function of applied electric field E; (c)(d) Measured reverse I-V curves and two devices fitting data based on the VRH model; (e) ln(J) versus (1/T)0.25 at reverse voltage of −5; (f)The schematic diagram of usub-SBD and utemp-SBD devices Schottky Fermi level jump to EVRH level at VR = 0.5 V.

(298–448 K, step is 25 K) based on Eq. (1),(2). The obtained ideality factor and ∅$_B$ values are shown in the Fig. 2(b). As the temperature increases from 298 K to 443 K, the barrier height of utemp-SBD and usub-SBD increases from 0.88 eV to 0.96 eV, and from 0.66 eV to 0.86 eV, respectively. At low temperature, the current is dominated by the low barrier regions because the carriers have no enough energy to cross over the high barrier regions. Then, the obtained effective ∅$_B$ at low temperature is smaller than that at higher temperature [24,25]. The η of the utemp-SBD decreases from 1.6 to 1.4, whereas the η of the usub-SBD remains nearly unchanged. It was found that there is a linear relationship between η and ∅$_B$ in utemp-SBD as shown in Fig. 2(c), implying a typical barrier inhomogeneous behavior [24,25]. Thus, compared to the usub-SBD, the utemp-SBD exhibits stronger temperature-dependent characteristics, indicating greater heterogeneity in barrier distribution [16,24]. This can be attributed to the fact that the Schottky contact

interface with a higher proportion of dislocations has a larger barrier height difference compared to the normal interface.

In Fig. 3(a), we conducted random testing of the reverse leakage characteristics of two devices of the same size on different substrates. It is observed that the device on the GaN substrate exhibits a more uniform leakage current compared to the device on the sapphire substrate. Fig. 3 (b),(c) shows the temperature-dependent reverse I-V characteristics of SBDs on both substrates. The curve trend can be divided into several voltage regions. For the utemp-SBD, region I is close to zero bias (V$_R$ < 1.5), region II ranges from −1.5 V to −12 V, region III spans from −12 V to −36 V, and region IV covers the range from −36 V to −40 V. Usub-SBD region I is close to zero bias (VR < 0.5), while region II is from −0.5 to −50 V. utemp-SBD shows a more complex leakage current conduction mechanism with more leakage channels. Leakage currents in quasi-vertical and all-vertical structures are primarily caused by
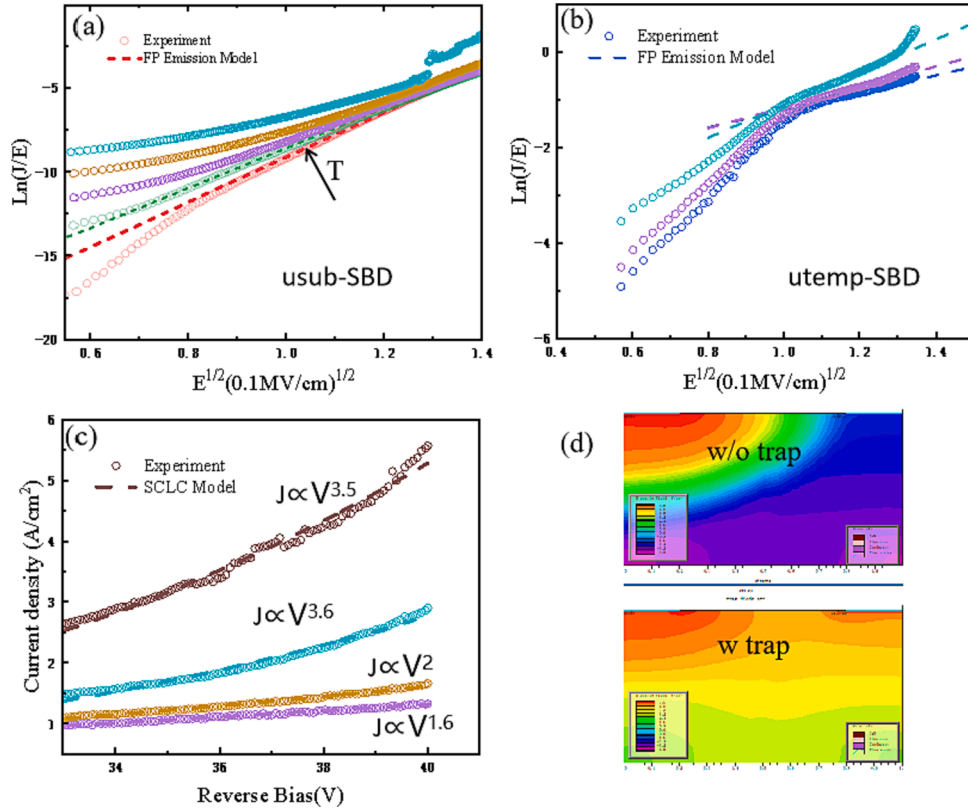
Fig. 5. (a),(b) Reverse ln (J/E) versus $E^{1/2}$ for usub-SBD and utemp-SBD, respectively; (c) SCLC model at the high reverse bias, following the relation of J-V^n; (d) Simulated electric field distribution in the usub-SBD and utemp-SBD at the VR of 40 V, respectively.

dislocations and defects in conductive layers [26,27]. However, it can be seen from the above results that the dislocation density and defect in the planar structure also have significant effects on the leakage current, because the biggest difference between the two devices in this work is the defect density in GaN.

As shown in Fig. 4(a) and (b), it can be observed that when the reverse voltage of the utemp-SBD is below 1.5 V and the usub-SBD is below 0.5 V, there is a linear relationship between LnJ (natural logarithm of current density) and V (voltage) at different temperatures (ranging from 298 K to 443 K). This linear relationship indicates that the dominant conduction mechanism of the leakage current is the thermionic emission (TE) model, which can be described by the equation [21,27]

$$\ln J = \ln(A^* T^2) - \frac{q\varnothing_B}{kT} + \frac{qV}{\eta kT} \qquad 3)$$

where η is ideality factor, The well-fitted results verify that the TE conduction is the dominant leakage mechanism [20].

When the reverse voltage of the utemp-SBD is between 1.5 V and 12 V (region II, corresponding to an electric field intensity of up to 0.1 MV/cm), the I-V curves measured at various temperatures exhibit excellent agreement with the theoretical fitting results based on the variable range hopping (VRH) model, described by the equation [21,26]

$$J_{VRH} = J(0)\exp\left(C\frac{qEa}{2kT}\left(\frac{T_0}{T}\right)^{-1/4}\right) \qquad 4)$$

the linear relationship between lnJ and E [Fig. 4(c)] indicates that the reverse leakage is mainly dominated by the variable range hopping (VRH) process [16], as shown in Fig. 4(d). For the usub-SBD, when the reverse voltage is between 0.5 V – 7 V (electric field intensity is 0.04–0.08 MV/cm), the usub-SBD shows a good linear relationship between lnJ and E, as shown in Fig. 4(e). Meanwhile, the lnJ as a function

of $1/T^{0.25}$ obtained from the experimental data under −5 V reverse bias exhibits a linear relationship as shown in Fig. 4(e), which confirms that the VRH conduction is the primary leakage mechanism for the usub-SBD between this region. Based on above observations, VRH mechanism begins to act as the dominant leakage mechanism at different voltage values (utemp-SBD and usub-SBD correspond to 1.5 V and 0.5 V, respectively) for two devices, which should be attributed to the different electric field intensity. Due to the higher carrier concentration and higher Schottky barrier height (SBH) of the GaN substrate, it transitions into the VRH mechanism (region II) at a reverse bias voltage of 0.5 V, with a higher electric field intensity of 0.04 MV/cm (the utemp-SBD reaches this value at −1.5 V). In region II, as the reverse bias increases, the electric field becomes higher, causing the energy band to steepen. This steeper VRH band (EVRH) results in a shorter hopping distance from the Schottky Fermi level to the VRH level in GaN [20]. Based on this theory, under the same reverse voltage, the usub-SBD has a steeper VRH band, indicating that electrons have a shorter hopping distance, making the usub-SBD more prone to the VRH conduction mechanism. This is illustrated in the schematic diagram in Fig. 4(f).

In the low-temperature range (323 K-373 K), when the V_R is raised above 7 V (E ∼ 0.08 MV/cm), ln(J/E) becomes linearly proportional to $E^{1/2}$, as depicted in Fig. 5 (a), implying that FP emission conduction-related leakage dominates the reverse leakage of the usub-SBD [21]. However, as the temperature increases (398 K–443 K), the dominant leakage mechanism changes from FP emission to VRH mechanism (Fig. 5(a) is observed in combination with Fig. 4(d)). This is different from the previous study [21]. FP emission involves charge carriers being trapped and then emitted to a continuous state, leading to the generation of dynamic current. As the temperature rises, the emission probability of trapped carriers increases [28]. However, in the case of the usub-SBD, the leakage current is mainly dominated by the VRH conduction mechanism, which is an abnormal phenomenon. We suspect that another VRH-related leakage channel, namely surface leakage,
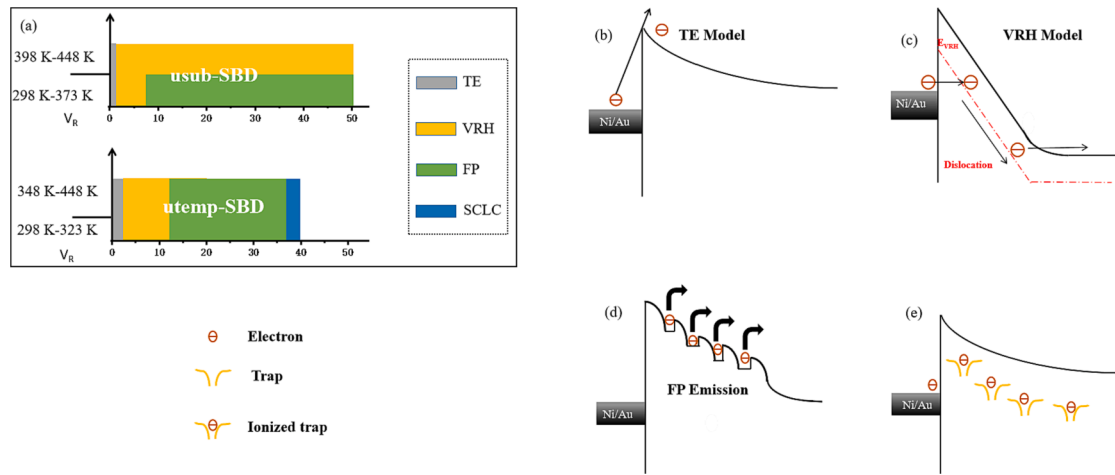
Fig. 6. (a) Schematic diagram of various leakage mechanisms for the usub-SBD and utemp-SBD under a reverse bias; The schematic diagram of reverse leakage based on the (b) TE, (c) VRH, (d) FP Emission, (e) SCLC models.

annihilates FP emission [29]. One of the possible mechanisms for surface current is two-dimensional variable hopping (2D-VRH) assisted by a high-density surface electronic state in GaN. This transition phenomenon is not observed in the utemp-SBD, as shown in Fig. 5(b). When the reverse voltage is between 12 V and 36 V (region III, E ~ 0.1—0.17 MV/cm), $\ln(J/E) \propto E^{1/2}$ indicates that the leakage mechanism of the utemp-SBD is dominated by FP emission. Compared to the free-standing GaN substrate, the higher defect density in GaN on sapphire enables FP emission to cover the temperature range.

As the V_R exceeds 36 V (E ~ 0.17 MV/cm) for the utemp-SBD, the leakage current increases more rapidly than the expected value based on the FP emission model as shown in Fig. 5(c). The well fittings based on the relation of J/V^n imply that the dominant leakage and breakdown mechanisms follow the space-charge-limited conduction SCLC model [20,30]. Under high electric field conditions, the high-density charged intrinsic traps in the space depletion region of the utemp-SBD can modulate the spatial electric field profile and affect the carrier transport process [20,31]. We used silvaco to simulate the electric field distribution inside diodes with and without trap. the acceptor trap energy level is 0.2 eV, and the acceptor trap concentration is 1e18/cm^3. Through simulation in Fig. 5(d), it is observed that different intrinsic defect densities make the two devices exhibit different electric field distributions under the same reverse voltage. In particular, the high-density intrinsic defect state of GaN-on-sapphire leads to a wider depletion region in the utemp-SBD (on the same field intensity scale). This promotes the leakage of a large number of acceptor defect ionization trapping carriers in the space charge region, which is in line with the space-charge-limited conduction (SCLC) leakage mechanism.

Fig. 6(a) illustrates the evolution of the various leakage mechanisms as the reverse voltage varies for both the utemp-SBD and the usub-SBD at different temperature. Under near-zero bias voltage, both devices exhibit a TE emission conductance mechanism. As the reverse voltage increases, due to the difference in Schottky barrier height, the larger electric field intensity in the usub-SBD depletion region makes usub-SBD first transform into VRH mechanism. With further voltage increase, the dominant leakage mechanism in the usub-SBD changes to FP emission and the 2D-VRH between the surface states of electrons in the process of temperature rise makes the leakage current dominant mechanism change to VRH. The dominant leakage mechanism in the utemp-SBD changes from FP emission to SCLC mechanism under the influence of intrinsic defects. The primary leakage mechanism model is shown in Fig. 6(b–e).

Conclusion

In summary, this work has conducted a comprehensive analysis of the phenomenon and underlying mechanisms of Schottky barrier diode (SBD) leakage on both free-standing and sapphire substrates through variable temperature current–voltage (IV) testing. The findings indicate that compared to the utemp-SBD, the usub-SBD exhibits a relatively simpler leakage mechanism and lower leakage current. The study analyzes the impact of leakage channels on the leakage mechanism of the device and provides a feasible analysis scheme for suppressing device leakage. These insights are valuable for the design and development of GaN-based power devices, especially in optimizing the performance and reducing leakage in Schottky barrier diodes. By understanding the different leakage mechanisms and their dependence on substrate choice and operating conditions, engineers and researchers can make informed decisions and design strategies to enhance device efficiency and reliability. This work contributes to the overall understanding of leakage mechanisms in GaN-based devices and provides guidance for future device design and optimization efforts.

Declaration of Competing Interest

The authors declare that they have no known competing financial interests or personal relationships that could have appeared to influence the work reported in this paper.

Data availability

Data will be made available on request.

Acknowledgement

References

[1] Anua N, Ahmed R, Shaari A, Ul Haq Bakhtiar, Mohamad Mazmira Binti. Adv Mater Res 2014;895:429–38.
[2] Valedbagi Sh, Mohammad Elahi S, Abolhassani MR, Fathalian A, Esfandiar A. Opt Mater 2015;47:44–50.
[3] Joubert D. Phys Rev B Condens Matter Mater Phys 1999;59:1758. [4] Yang M, Chang B, Hao G, Wang H, Wang M. Optik 2015;126:3357–61.

[4] Ambacher O, Smart J, Shealy JR, Weimann NG, Chu K, Murphy M, et al. Twodimensional electron gases induced by spontaneous and piezoelectric polarization charges in N- and Ga-face AlGaN/GaN heterostructures. J Appl Phys 1999;85(6):3222–33.

[5] Hariya A, Koga T, Matsuura K, Yanagi H, Tomioka S, Ishizuka Y, et al. Circuit design techniques for reducing the effects of magnetic flux on GaN-HEMTs in 5-MHz 100-W high power-density LLC resonant DC-DC converters. IEEE Trans Power Electron 2017;32(8):5953–63.

[6] Aminbeidokhti A, Dimitrijev S, Han J, Chen X, Xu X. The power law of phonon-limited electron mobility in the 2-D electron gas of AlGaN/GaN heterostructure. IEEE Trans Electron Devices 2016;63(5):2214–8.

[7] Huang S, Liu X, Wang X, Kang X, Zhang J, Fan J, et al. Ultrathin-barrier AlGaN/GaN heterostructure: a recess-free technology for manufacturing high-performance GaN-on-Si power devices. IEEE Trans Electron Devices Jan 2018;65(1):207–14.

[8] Wang Z-X, Du L, Liu J-W, Wang Y, Jiang Y, Ji S-W, et al. Breakdown voltage enhancement in GaN channel and AlGaN channel HEMTs using large gate metal height. Chin Phys B 2020;29(2):027301.

[9] Jiang H, Zhu R, Lyu Q, Lau KM. High-voltage p-GaN HEMTs with off-state blocking capability after gate breakdown. IEEE Electron Devices Lett 2019;40(4):530–3.

[10] Radhakrishna U, Choi P, Antoniadis DA. Facilitation of GaN-based RF- and HV-circuit designs using MVS-GaN HEMT compact model. IEEE Trans Electron Devices Jan 2019;66(1):95–105.

[11] Pushpakaran BN, Subburaj AS, Bayne SB. Commercial GaN-based power electronic systems: a review. J Electron Mater 2020;49(11):6247–62.

[12] Mahajan, S.S. et al. Gate Leakage Current Suppression in AlGaN/GaN HEMT by RTP Annealing. In: Jain, V., Verma, A. (eds) Physics of Semiconductor Devices. Environmental Science and Engineering. Springer, Cham. 2014.

[13] Liu H-Y, Chou B-Y, Hsu W-C, Lee C-S, Sheu J-K, Ho C-S. Enhanced AlGaN/GaN MOS-HEMT Performance by using hydrogen peroxide oxidation technique. IEEE Trans Electron Devices 2013;60(1):213–20.

[14] Palacios T, Suh C-S, Chakraborty A, Keller S, DenBaars SP, Mishra UK. High-performance E-mode AlGaN/GaN HEMTs. IEEE Electron Device Lett 2006;27(6):428–30.

[15] Saito W, Kuraguchi M, Takada Y, Tsuda K, Omura I, Ogura T. High breakdown voltage undoped AlGaN-GaN power HEMT on sapphire substrate and its demonstration for DC-DC converter application. IEEE Trans Electron Devices 2004;51(11):1913–7.

[16] Hsu J W P, Manfra M J, Molnar R J, et al. Direct imaging of reverse-bias leakage through pure screw dislocations in GaN films grown by molecular beam epitaxy on GaN templates. Applied physics letters. 2002,81(1):79-81.

[17] Li D S, Chen H, Yu H B, et al. Dependence of leakage current on dislocations in GaN-based light-emitting diodes. Journal of applied physics. 2004,96(2):1111-1114.

[18] Zhang Y, Wong H-Y, Sun M, Joglekar S, Yu L, Braga NA, et al. IEEE Int Electron Devices Meeting (IEDM) 2015:900.

[19] Yuhao Zhang, Min Sun, Hiu-Yung Wong, Yuxuan Lin, Srivastava P, Hatem C, et al. Origin and control of OFF-state leakage current in GaN-on-Si vertical diodes. IEEE Trans Electron Devices 2015;62(7):2155–61.

[20] X. Guo, Y. Zhong, X. Chen, Y. Zhou, S. Su, S. Yan, J. Liu, X. Sun, Q. Sun and H. Yang. Reverse leakage and breakdown mechanisms of vertical GaN-on-Si Schottky barrier diodes with and without implanted termination. Appl. Phys. Lett. 2021,118, 243501. Jiabo Chen , Zhihong Liu , Haiyong Wang.

[21] Chen J, Liu Z, Wang H, Song X, Bian Z, Duan X, et al. Determination of the leakage current transport mechanisms in quasi-vertical GaN–on–Si Schottky barrier diodes (SBDs) at low and high reverse biases and varied temperatures. Appl Phys Express 2021;14(10):104002.

[22] Yonenaga I. dislocation behavior in heavily impurity doped Si. Scr Mater 2001;45 (11):1267–72.

[23] Davidov SY, Tikhonov SK. surface donor states induced by metal atoms adsorbed on wide-gap semiconductors. Phys Solid State 1995;37(9):1514–6.

[24] Mark C. Lonergan, Frank E. Jones. Calculation of transmission coefficients at nonideal semiconductor interfaces characterized by a spatial distribution of barrier heights. J. Chem. Phys. 2001, 115(1), 433–445.

[25] Sang, Liwen, Bing, et al. Initial leakage current paths in the vertical-type GaN-on-GaN Schottky barrier diodes. Applied physics letters. 2017(111-12).

[26] Dong-Pyo Han, Chan-Hyoung Oh, Hyunsung Kim, Jong-In Shim, Kyu-Sang Kim, Dong-Soo Shin. Conduction mechanisms of leakage currents in ingan/gan-based light-emitting diodes. IEEE Trans Electron Devices 2015;62(2):587–92.

[27] Chen J, Bian Z, liu Z, Zhu D, Duan X, Wu Y, et al. Effects of thermal annealing on the electrical and structural properties of Mo/Au schottky contacts on n-GaN. J Alloy Compd 2021;853:156978.

[28] Simmons JG. conduction in thin dielectric films. J Phys D Appl Phys 1971;4(5):613–57.

[29] Kotani J, Tajima M, Kasai S, et al. Mechanism of surface conduction in the vicinity of Schottky gates on AlGaN/GaN heterostructuresn. Appl Phys Lett 2007;91(9):3501.

[30] Xu J, Liu X, Xie B, Hao Y, Wen CP, Wei J, et al. correlation between reverse leakage current and electric field spreading in gan vertical sbd with high-energy ion implanted guard rings. IEEE Trans Electron Devices 2023;70(4):1745–50.

[31] Nicholls JR, Dimitrijev S, Tanner P, Han J. The role of near-interface traps in modulating the barrier height of sic schottky diodes. IEEE Trans Electron Devices 2019;66(4):1675–80.